Modeling the barotropic circulation on Inner Ambon Bay

Article *in* International Journal of Oceans and Oceanography · January 2016

CITATIONS
6

READS
335

4 authors, including:

Yunita Noya
Pattimura University
19 PUBLICATIONS **50** CITATIONS
SEE PROFILE

Tri Prartono
Bogor Agricultural University
45 PUBLICATIONS **359** CITATIONS
SEE PROFILE

International Journal of Oceans and Oceanography
ISSN 0973-2667 Volume 10, Number 2 (2016), pp. 265-286

http://www.ripublication.com

Modeling the Barotropic Circulation on Inner Ambon Bay

Yunita A. Noya[a, b*], Mulia Purba[a], Alan F. Koropitan[a], and Tri Prartono[a]

[a]Department of Marine Science and Technology, Bogor Agricultural University (IPB)
Kampus IPB Darmaga, Bogor 16680, Indonesia
[b]Faculty of Fisheries and Marine Science, Pattimura University (UNPATTI)
Kampus UNPATTI, Ambon 97235, Indonesia

Abstract

Numerical model of MIKE 3 FM has been utilized in order to investigate barotropic circulation in the Inner Ambon Bay, particularly the influence of narrow channel between inner and outer parts of the bay. The comparison between model result and observation has similar pattern for the tidal elevation. Model results clearly show two eddies in the inner part with opposite direction each other (cyclonic and anti-cyclonic) and barotropic condition prevailing away from the channel in the deepest point of bay. It seems around of the channel, barotropic approximation does not work very well. The present research also considers the flow of river and boundary discharge for northwest and southwest monsoon seasons and discusses their behavior in the Inner Ambon Bay.

Keyword: Inner Ambon Bay, numerical model, barotropic circulation, eddy, river and boundary discharge.

I. INTRODUCTION

Inner Ambon Bay (IAB) is a semi-enclosed water and has a narrow channel that connecting IAB to Ambon Bay [1, 2]. Generally IAB has three important aquatic ecosystems such as mangrove, seagrass, and coral reef. This makes IAB as fishing ground for local fishermen, marine-culture and ecologically, IAB is a place for sheltering, feeding and breeding ground for many species of pelagic fish [3]. IAB also is the estuary for several rivers that flow through the years. It's affected the mechanisms of water dynamic and chemical-physical characteristics of the waters such as temperature, salinity, dissolved oxygen, phosphate, and nitrate. The surface layer is strongly influenced by the fresh waters inflow of the river that empty into IAB

[1, 2, 4, 5]. The rivers inflow carrying the sediment debris, which are the result of the erosion a soil particle by run-off rain into water bodies and boils down to IAB waters. This has led to the problem of sedimentation in coastal IAB [6, 7].

Sedimentation problems not only affect aquatic ecosystems such as mangrove [8], seagrass [9], and yet sedimentation can change the morphology of waters such as generate sandbar or other topography shape. Sedimentation is very influential on water circulation patterns, especially on semi-enclosed and shallow waters. As in seamount in the Bay of Biscay, the circulation flow pattern is anti-cyclonic eddies caused by the friction of flow at the side of seamount [10]. The same was found in the Gulf of Mexico, the flow of current through the ravine (canyon) at a depth of 150m generate anti-cyclonic eddies [11]. Whereas in other research in the Bay of Biscay barotropic circulation strongly occurred at a depth of 60m during the summer and autumn in the southern gulf [12]. The flow varies seasonally due to average kinetic energy is greater in the summer [13]. This shows that the barotropic circulation is occurred more in shallow waters. To understand the barotropic circulation we used numerical equations of two and three dimension in hydrodynamic models, to compute parameters such as current magnitude and direction for which wind and tidal are used as the driving forces [14, 15].

In recent decades, the hydrodynamic modeling of shallow waters, semi-enclosed waters and ocean is more advanced. There are different kinds of hydrodynamic models that has been produced to examine and interpreting the patterns of circulation in the semi-enclosed waters such as: ROMS, HAMSOM, FVCOM, ELCIRC, and MIKE 3 FM. The Regional Ocean Modeling System (ROMS) has been used to analyzed the configuration and sensitivity tidal waters baroclinic and barotropic circulations on Monterey Bay – California [16]. Hamburg shelf ocean model (HAMSOM) has modeled water circulation patterns in the semi-enclosed "Bohai Sea" by considering the influence of the tides, wind and baroclinic force [17]. Finite volume coastal ocean model (FVCOM) has used a structured grid horizontally to increase the efficiency and effectiveness of models [18]. Eulerian-Lagrangian finite difference/finite volume model (ELCIRC) is designed to simulate the circulation of the mass flow of water from the rivers to scale marine waters [19]. Danish hydraulic institutes-Modelling (DHI–MIKE) is a three-dimensional hydrodynamic model. This model is used to view the channel circulation at Songdo Waterfront [20]. This present study used the 3-D finite volume hydrodynamic model, MIKE 3 FM. The primary aim of this modeling study is to understand the patterns of water circulation on IAB and how the change of seasons affects the circulation patterns.

II. METHODS

2.1 Study area

Inner Ambon Bay (IAB) is a part of Ambon Bay located on the Ambon Island, Moluccas Province, Indonesia. Geographically, the study area lies on 128^0–129^0 E and 3^0–4^0 S [21]. IAB has a fairly narrow channel with a width of ±800m and the

average depth at the channel is about 12m. The maximum depth is at a point closer to the brink of around 42m in the form of topography is essentially like a bowl. On the east to southeast bay depth of 35m, while on the side of west to northwest bay the depths only reached 10-25m. The IAB has average depth of about 25-30m and there are ±8 permanent rivers that flow throughout the year and ±3 temporal river which flows only during the rainy season (Figure 1).

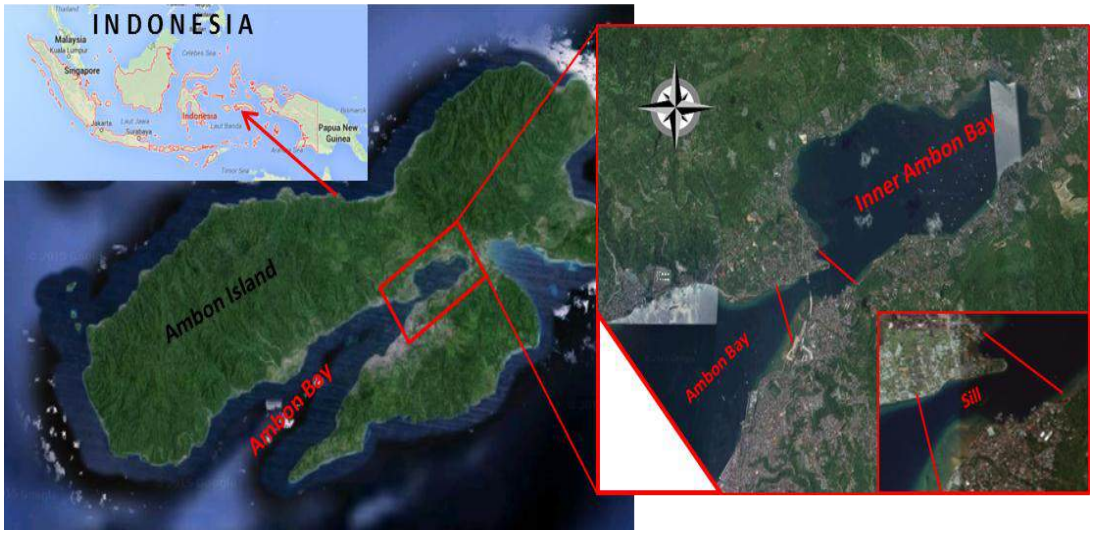

Figure 1: Map of Inner Ambon Bay Moluccas Province showing the research sites

2.2 Design models and boundary conditions

Design of the model in this study is a barotropic models and using mesh adjustment, because MIKE 3 FM is a model with a flexible mesh system. Setting triangular mesh generated by MIKE Zero and divides the research sites into three section (Figure 2), i.e. Inner Ambon Bay, Sill (Poka-galala), Ambon Bay, with total domains is 44178 elements and 5321 nodes (Table 1).

Table 1: Triangular mesh of research sites at three sections

No.	Section	Size mesh (m)	Nodes	Element
I.	Inner Ambon Bay (IAB)	100 x 100	2055	25853
II.	Sill (Poka-galala)	50 x 50	2734	12841
III.	Ambon Bay	200 x 200	532	5484

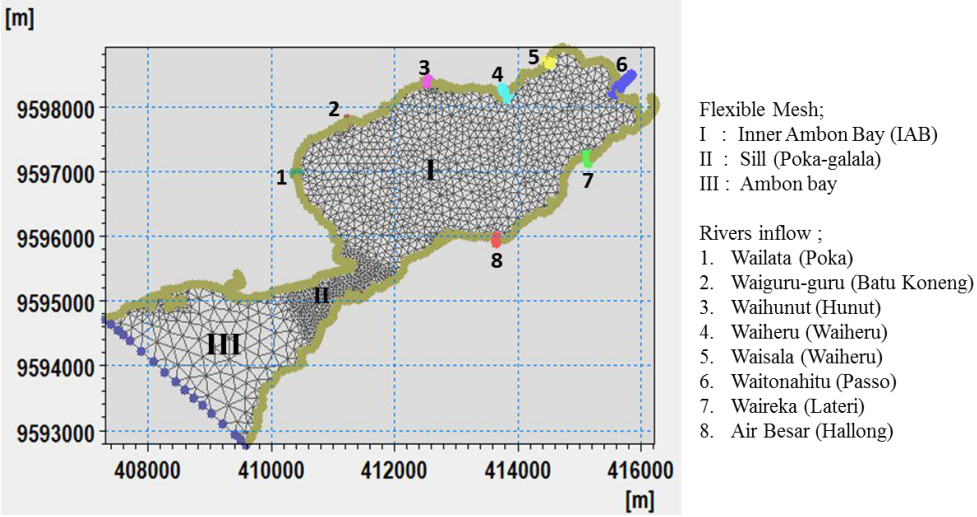

Figure 2: Mesh and boundary conditions at each sections.

In this research models we used barotropic conditions considering that IAB is semi-enclosed and shallow waters, which mean that the ocean waters are mixed and produced homogeneous layer. The density is not increased with depth and the isobaric surface parallel to the surface of the sea but also with a constant density. We used tidal as hydrodynamic driving force while the wind parameters is been ignored. In previous research on the circulation of IAB showed that the dominant hydrodynamic parameter is tidal currents [22]. Similar research in the Gulf of Biscay and the Gulf of Mexico concluded that tidal currents were the dominant parameters [11, 12, 13]. While wind parameters can be ignored because the condition of gulf waters is tend to be obstructed by hills, therefore the wind forces is not too influential [7]. However we append inflow streams as input in the models i.e. wailata (Poka), waiguru-guru (Batu.koneng), waihunut (Hunut), waiheru (Waiheru), waisala (Waiheru), waitonahitu (Passo), waireka (Lateri), and air besar (Halong) (Figure 2). The permanent rivers inflow were used as water input because the debit were constant and influence the circulation system on IAB.

Tidal harmonic components (M2, S2, K1, and O1) were used as input for tidal potential in MIKE 3 FM menu model, because it was recorded as a dominant tidal component of Indonesia waters [23, 27]. Horizontal eddy viscosity coefficient is using Smagorinsky constants (0.28) and Log Law constants for vertical eddy viscosity in the maximum ranges 0.4 m^2/s. The bed resistance is using Quadratic drag coefficient (0.03) [24].

The boundary condition for hydrodynamic model is water elevation (sea level) and rivers inflow. Open boundary is area frontier of the Ambon Bay and estuary in area of IAB, for a closed boundary is the coastline of the study area (land boundary) which is we assuming a vertical wall that doesn't allow the mass waters passing through or in other side the velocity in the direction perpendicular to coastline is zero ($u = v = 0$).

2.3 Hydrodynamic model equations

The equations we used in this models are a three-dimensional equation of incompressible Reynolds averaged Navier-Stokes equations, subject to the assumptions of Boussinesq and of hydrostatic pressure [24].

The continuity equation is written as;

$$\frac{\partial u}{\partial x}+\frac{\partial v}{\partial y}+\frac{\partial w}{\partial z}=S \tag{1}$$

The momentum equations for the -x- and -y- component, respectively;

$$\frac{\partial u}{\partial t}+\frac{\partial u^2}{\partial x}+\frac{\partial vu}{\partial y}+\frac{\partial wu}{\partial z}= fv-g\frac{\partial \eta}{\partial x}-\frac{1}{\rho_0}-\frac{\partial p_a}{\partial x}-\frac{g}{\rho_0}\int_z^\eta \frac{\partial \rho}{\partial x}dz+F_u+\frac{\partial}{\partial Z}\left(v_t\frac{\partial u}{\partial t}\right)+u_s\,S \tag{2}$$

$$\frac{\partial v}{\partial t}+\frac{\partial v^2}{\partial x}+\frac{\partial uv}{\partial y}+\frac{\partial wv}{\partial z}= -fu-g\frac{\partial \eta}{\partial y}-\frac{1}{\rho_0}-\frac{\partial p_a}{\partial y}-\frac{g}{\rho_0}\int_z^\eta \frac{\partial \rho}{\partial y}dz+F_v+\frac{\partial}{\partial Z}\left(v_t\frac{\partial u}{\partial t}\right)+v_s\,S \tag{3}$$

where t is the time; x, y and z are the Cartesian co-ordinates; η is the surface elevation; d is the still water depth; $h=\eta+d$ is the total water depth; u, v and w are the velocity components in the x, y and z direction; $f=2\Omega\sin\phi$ is the Coriolis parameter (Ω is the angular rate of revolution and ϕ the geographic latitude); g is the gravitational acceleration; ρ is the density; v_t is the vertical turbulent (or eddy) viscosity; p_a is the atmospheric pressure; ρ_0 is the reference density. S is the magnitude of the discharge due to point source and ($u_s v_s$) is the velocity by which the water is discharged into the ambient water.

The horizontal stress terms are described using a gradient-stress relation, which is simplified to;

$$F_u=\frac{\partial}{\partial x}\left(2A\frac{\partial u}{\partial x}\right)+\frac{\partial}{\partial x}\left(A\left(\frac{\partial u}{\partial y}+\frac{\partial v}{\partial x}\right)\right) \tag{4}$$

$$F_v=\frac{\partial}{\partial x}\left(A\left(\frac{\partial u}{\partial y}+\frac{\partial v}{\partial x}\right)\right)+\frac{\partial}{\partial y}\left(2A\frac{\partial v}{\partial y}\right) \tag{5}$$

where A is the horizontal eddy viscosity.

The surface and bottom boundary condition for ; u, v and w are;

$$\frac{\partial \eta}{\partial t}+u\frac{\partial \eta}{\partial x}+v\frac{\partial \eta}{\partial y}-w=0,\quad \left(\frac{\partial u}{\partial z},\frac{\partial v}{\partial z}\right)=\frac{1}{\rho_0 v_t}\left(\tau_{sx},\tau_{sy}\right) \tag{6}$$

where $\left(\tau_{sx},\tau_{sy}\right)$ are the x and y components of bottom stresses.

The bottom stress;

$\vec{\tau}_b = (\tau_{bx}, \tau_{by})$, is determined by a quadratic friction law [24]

$$\frac{\vec{\tau}_b}{\rho_0} = C_f \vec{u}_b |\vec{u}_b| \quad (10)$$

where C_f is the drag coefficient and $\vec{u}_b = (u_b, v_b)$ is the flow velocity above the bottom. The friction velocity associated with the bottom stress is given by;

$$U_{\tau b} = \sqrt{c_f |u_b|^2} \quad (11)$$

$$c_f = \frac{1}{\left(\frac{1}{\kappa} \ln\left(\frac{\Delta z_b}{z_0}\right)\right)^2} \quad (12)$$

where $\kappa = 0.4$ is the von Karman constant and z_0 is the bed roughness length scale. When the boundary surface is rough z_0 , depends on roughness height, κ_s

$$z_0 = M \kappa_s \quad (13)$$

where m is approximately 1/30.

$$M = \frac{25.4}{{k_s}^{1/6}} \quad (14)$$

III. RESULT

3.1 Models verification

The parameter used for verification in this research is the sea level and tidal current. The comparison between the models result (blue line) and mooring (red line) of sea level (Figure 3) shows similarities to the up-downs pattern of tidal fluctuations. However, interval time between points 100-200 during the neap tides phase there are slightly different on the magnitude. As proposed in modeling of dynamics tides change in the Gulf of Jiaozhou, the event of neap tide rendering the tidal propagation delayed thus affecting to a magnitude of tidal [25]. We conclude that the sea level fluctuations between the model and mooring results are compared well.

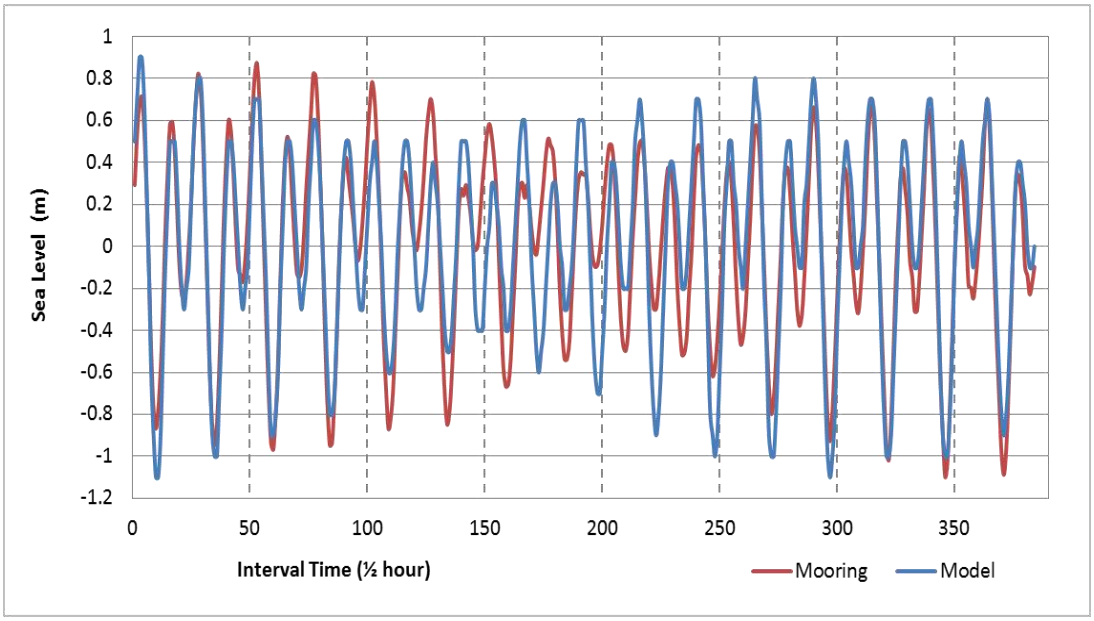

Figure 3: Sea level comparison between the model result (blue) and mooring (red)

The mooring result (red dot) of tidal current in the rainy season (July 2011) generally showed patterns of the North-South flows, however the direction of V-velocity dominant to the south and for U-velocity is dominant to the southwest (Figure 4a). Also for dry season (January 2012) generally indicated the East-West direction, but the V-velocity dominant is to the south and for U-velocity is varied between southeast until southwest (Figure 4b). The result of previous studies at Ambon Bay obtained that directions of flows varied between the southeast to southwest and dominant to the South, which is similar with the mooring results [22]. The flow movement patterns of the models results (blue dot) shows the same direction as for mooring, but the current magnitude between both results reveals slightly differences. The research in Daya Bay-China also shows a slight difference between the current magnitudes of model and mooring results. It was thought that the difference is due to the complexity of bay geometry [26]. The slight differences of tidal currents magnitude at the point of comparison especially occurred during the dry season when the mass of water slightly decreased. This difference indicates that flow nearby the sill is affected by the topography for which the barotropic model is not a good assumption there but around the deepest Ambon Bay may works very well. It is anticipated that baroclinic condition may be suitable around the sill.

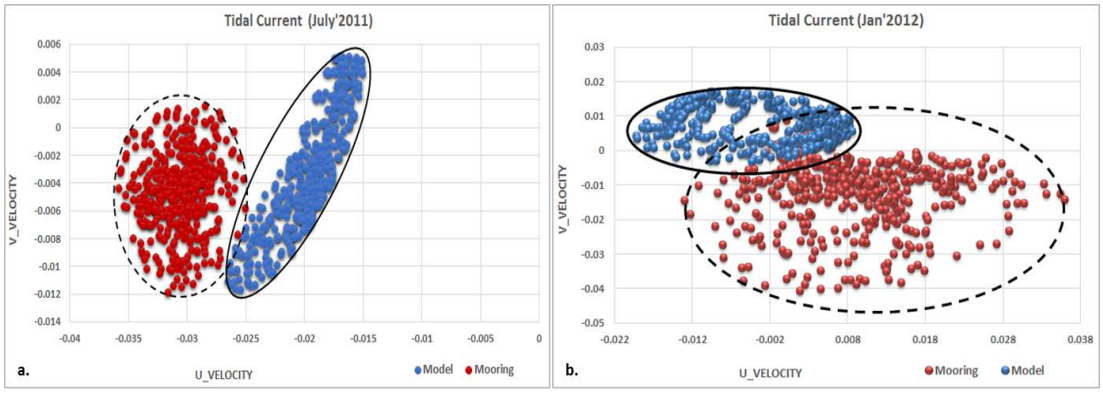

Figure 4: Tidal current comparison of model and mooring results; a. Tidal current on rainy season (July 2011), b. Tidal current on dry season (January 2012)

3.2 Simulation in rainy season

During the rainy seasons discharge of rivers increased and influenced the volumes of IAB [7]. In this research we recorded the average rainfall and was found around 22.3mm/day and supplied the fresh water for 8 rivers (Table 2) with 0.953m^3/s of discharge inflow to IAB. Table 2 shows the maximum discharge flow of rivers is in Waitonahitu about 2.74m^3/s, this rivers is affecting the current flows around passo area (end of IAB). The minimum discharge of rivers is at Air Besar (Halong area) around 0.085m^3/s, which is the closest river to the sill. The exchange of water mass through the sill is in accordance to the tidal phase and basically the main causes of circulation on IAB are tidal. At phase of ebb tide and low tide the waters mass flow is moving out of IAB to Ambon Bay. While at the phase of flood tide and high tide the waters mass flow is entering from Ambon Bay to IAB. The previous studies revealed same thing about the entry-exit of current flow and water mass at IAB [5, 22, 29, 30].

Table 2: Average river discharge in Inner Ambon Bay

River name	Area	Average River Discharge (m^3/s)	
		Rainy Season	Dry Season
Wailata	POKA	1.470	0.946
Waiguru-guru	BATU KONENG	0.462	0.236
Waihunut	HUNUT	0.677	0.346
Waiheru	WAIHERU	0.786	0.694
Waisala	WAIHERU	0.470	0.281
Waitonahitu	PASSO	2.749	1.772
Waireka	LATERI	0.923	0.336
Air besar	HALONG	0.085	0.038
Total Discharge		0.953	0.581

The current speed in rainy season at phase of ebb tide (Figure 5) shows that the mass of water moving from around Passo waters (end of bay), the current flow tends to be strong along a side of Waiheru waters with average flow velocity 0.016m/s. It seems that the water mass is driven by the inflow of Waisala and Waiheru Rivers, and moving towards Lateri waters. Moreover, inflow of Waireka River probably provide a dominant pressure toward Passo waters. When flow entered the channel, the flow rate is increasing to around 0.55-0.45m/s. The previous researches obtain the same result that flow velocity rise at the channel to about 0.5m/s [5, 22, 28, 29, 30]. The dominant of current flow is along west side of channel because it is deepest than east side of channel. While the average of current speed in Ambon Bay is 0.03m/s at surface layer (0.25m) and 0.01m/s in 30m of depth (Figure 5a, 5c).

On phase of low tide (Figure 6) it seen there are two horizontal eddy i.e. anti-clockwise eddy [yellow arrow] occurs around the Passo waters (end of bay) and clockwise eddy [red arrow] occurs around the Hunut waters. The clockwise eddy around Hunut waters probably driven by the dominant flow from Halong waters with average speed about 0.018m/s that headed to the waters around Batu koneng, This the flow divided into two parts i.e. the dominant flow toward Poka waters and the rest of the flow turned into Hunut waters. The turned current flow of Hunut water forming the horizontal clockwise eddy even with fairly slow velocity < 0.01m/s. Overall, both of horizontal eddy appeared in the surface layer (0.25m) to 20m (Figure 6a, 6b, 6c), while at 30m of depth (Figure 6d) the eddys disappearing probably due to constriction of the topography. The horizontal eddy formation such as this obtained in results of circulation models in Gulf of Patras (Greece), because of tides [31, 32] and the influence of coastline morphology as well as topography configuration [34, 35].

The waters mass with flow velocity about 0.03-0.01m/s from Ambon Bay toward IAB at flood tide phase is given in Figure 7. The flow rate is increasing when approaching the channel around 0.09-0.06m/s. After reaches the channel flow velocity become 0.7-0.5m/s, probably due to the flow is constricted by the narrow sill. This is the maximum flow value in tide phase and causing a turbulent (wake) around sill of IAB. The maximum flow from sill toward the deepest point of IAB generated the horizontal eddys (wake), it shows at 20 of depth (Figure 7c). In theory; the wake occur when a flow passes through the barrier or wall (in this case the barrier is the shallow sill), wake is the turbulent in front or behind the barrier or wall in a stream. Simple assumption, that the wake can be divided into wall region (close to the wall and mixing region) spreading from the top of the obstacle [33]. The inflow to IAB is dominant along the Halong waters and after through the Halong waters the current flow is weakened as it reaches the middle of bay with the flow velocity between 0.05-0.02m/s. Current vector indicates the flow of middle bay towards Batu koneng and Hunut waters, then turned again to the center of bay (between Waiheru and Lateri) due to the flow is collided with the shoreline around Waiheru there is slightly protruded to the center of bay. Although, the slow current flow (0.03-0.01m/s) but the water mass around Lateri waters move toward to Passo waters (end of bay).

At phase of the high tide (Figure 8) shows the water mass flow dominant from middle Ambon Bay toward IAB. Overall, the current vector in Ambon Bay is divided into two parts; the flow dominant leading to IAB (Figure 8a, 8b) while the other current flow towards opposite direction which is to the open boundary condition (exit of Ambon Bay) (Figure 8c, 8d) with average flow velocity 0.011m/s. The current flow entering through the channel with the flow velocity increased about 0.15-0.06m/s, this velocity constant until the flow reach Halong. The current flow through of Halong waters and turned to the middle of bay, heading toward Batu koneng and Hunut waters. Generally, the current flow that occurs in IAB in this phase is similar to the flow at ebb tide phase. However, the differences on the horizontal eddy: at the surface layers (0.25m) where two anti-clockwise eddy were formed. One is in center of the bay and the other is surrounding Passo waters (Figure 8a). Moreover at a depth of 10-20m clockwise eddy appeared in the waters between Halong and Lateri. The occurance of this eddy is probably due to the dominant water mass flow toward Lateri waters and divided into two parts i.e. half part flow towards Halong waters and another part towards Passo waters. The flow toward Passo probably created anti-clockwise eddy at Passo waters (Figure 8b, 8c). Eddies commonly occur in coastal zone [36] and can be formed by obstruction from sea floor topography [37].

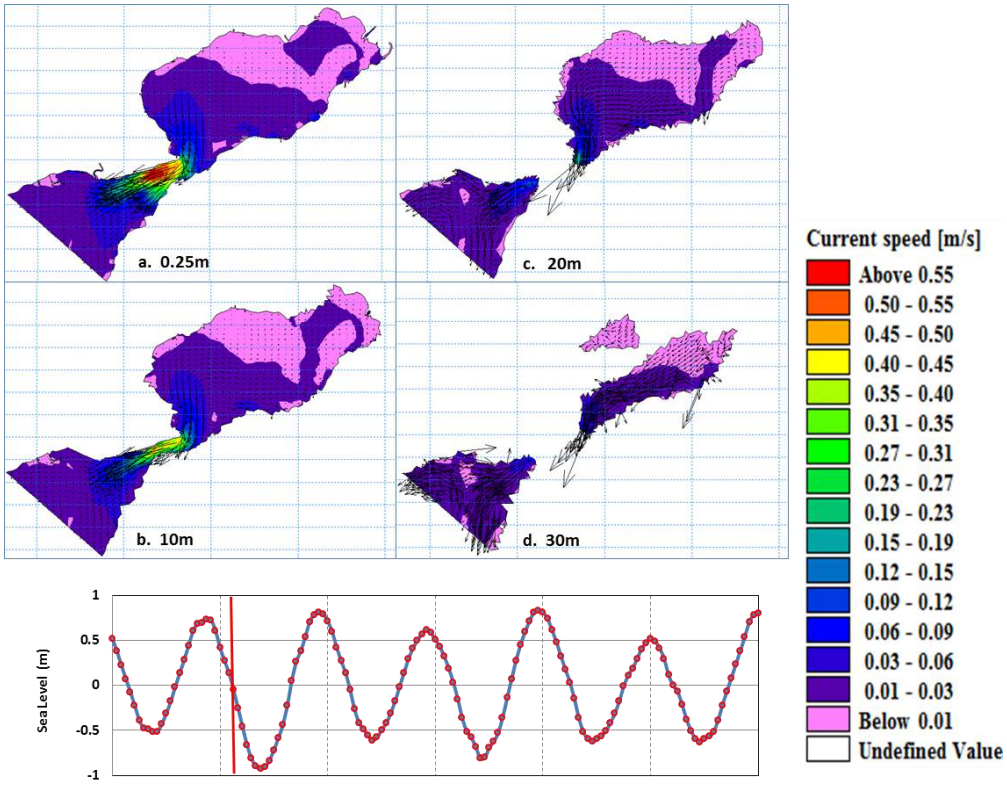

Figure 5: Current speed in the rainy season, phase ebb tide (in the depth of): a). 0.25m, b). 10m, c). 20m, d). 30m

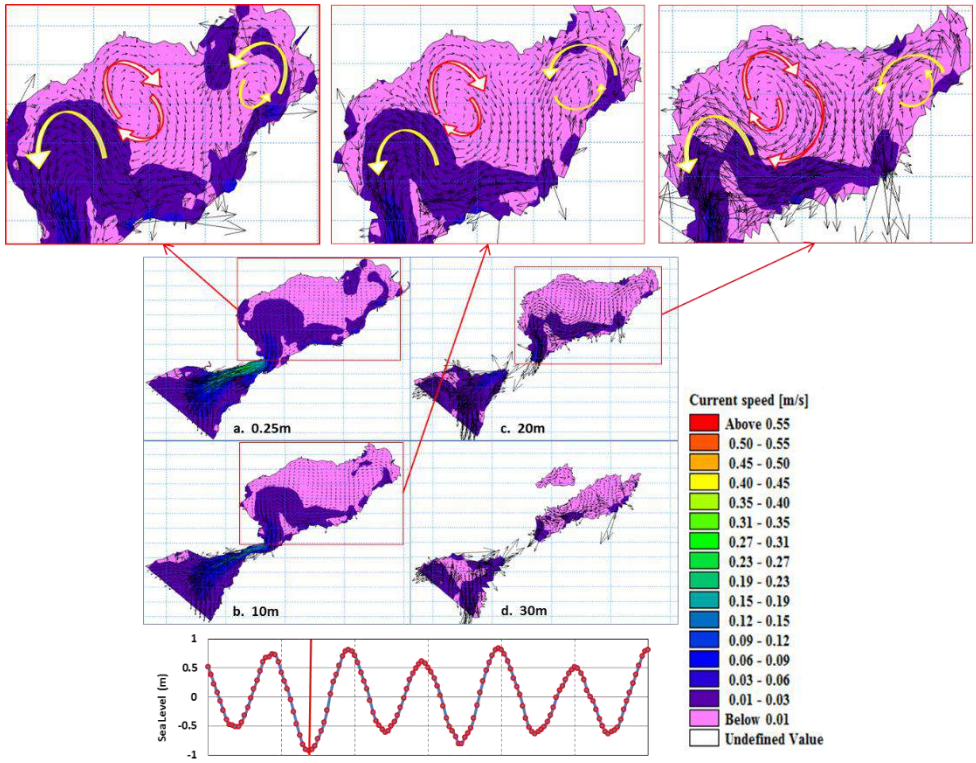

Figure 6: Current speed in the rainy season, phase low tide (in the depth of): a). 0.25m, b). 10m, c). 20m, d). 30m

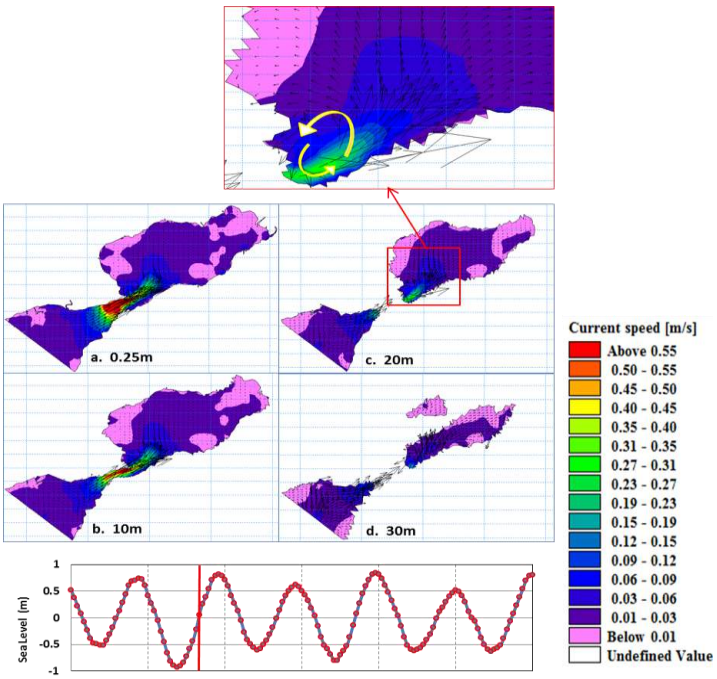

Figure 7: Current speed in the rainy season, phase flood tide (in the depth of): a). 0.25m, b). 10m, c). 20m, d). 30m

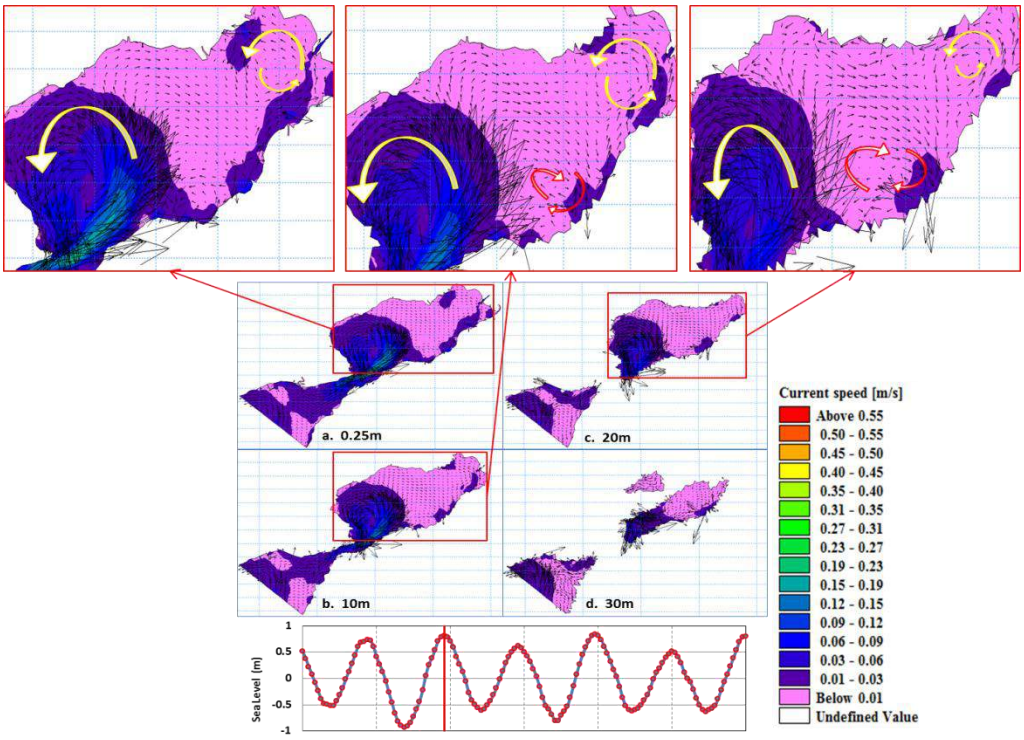

Figure 8: Current speed in the rainy season, phase high tide (in the depth of): a). 0.25m, b). 10m, c). 20m, d). 30m

The cross section at phase ebb tide (about 0.245m/s)(Figure 9a) shows the average flow velocity come out of the IAB to Ambon Bay thru the channel is higher than on low tide (0.082m/s) (Figure 9b). Moreover, these flows affecting the barotropic distance, on ebb tide the barotropic distance is around 4490m, while at low tide the barotropic distance is about 4510m for which the distance is from the middle of the bay to Passo waters (end of bay) (Table 3). There are indications if the flow discharges out of the IAB are compared, then barotropic distance can be longer if the flows getting smaller. In Figure 9b the vertical anti-clockwise eddy around Ambon Bay (in front of channel) at 40m of depth, (if we compared with Figure 6d) it appears that water mass from Ambon Bay entering to IAB (from open boundary conditions). The waters mass flow at the depth of 40 m does not reach the channel due to shallow bottom topography, and at surface layer the inflow heading out from IAB (meaning the inflow is opposite direction to the flow on 40m depth). Vertical eddy formed in front of the channel on the Ambon Bay site. Nearby the sill, upwelling motion produce the vertical eddies and trigger by this unstable structure [28, 36].

In phase of flood tide are (Figure 10) shows the distance of barotropic condition is about 3010m and 3060m at the phase of high tide (Table 3). Barotropic condition at this phase is shorter than phase of ebb tide and low tide. This is probably because of the flow water mass that enters to IAB will be reflected by the deepest point of bay and may produce baraclinic condition around the sill, as a result the shorter distance

of barotropic occurred. At phase high tide (Figure 10b) shows the vertical clockwise eddy in Ambon Bay (in front of channel) occurred at depth of 20m of depth. This eddy happen cause the current flow from Ambon Bay entering to IAB with flow velocity about 0.03-0.01m/s, at surface layer (0.25m) until 20m of depth (see Figure 8a, 8b, 8c).

Table 3: Average of current velocity and barotropic distance

Time	Average of Current velocity (m/s)			Distance of barotropic (m)
	0.25-30m		0.25-10m	
Rainy Season	**Ambon Bay**	**IAB**	**Sill**	
Ebb tide	0.023	0.016	0.245	4490
Low tide	0.018	0.009	0.082	4510
Flood tide	0.022	0.021	0.329	3010
High tide	0.011	0.017	0.060	3060
Dry Season				
Ebb tide	0.023	0.015	0.246	4060
Low tide	0.014	0.007	0.027	3060
Flood tide	0.014	0.013	0.193	3560
High tide	0.009	0.014	0.028	3040

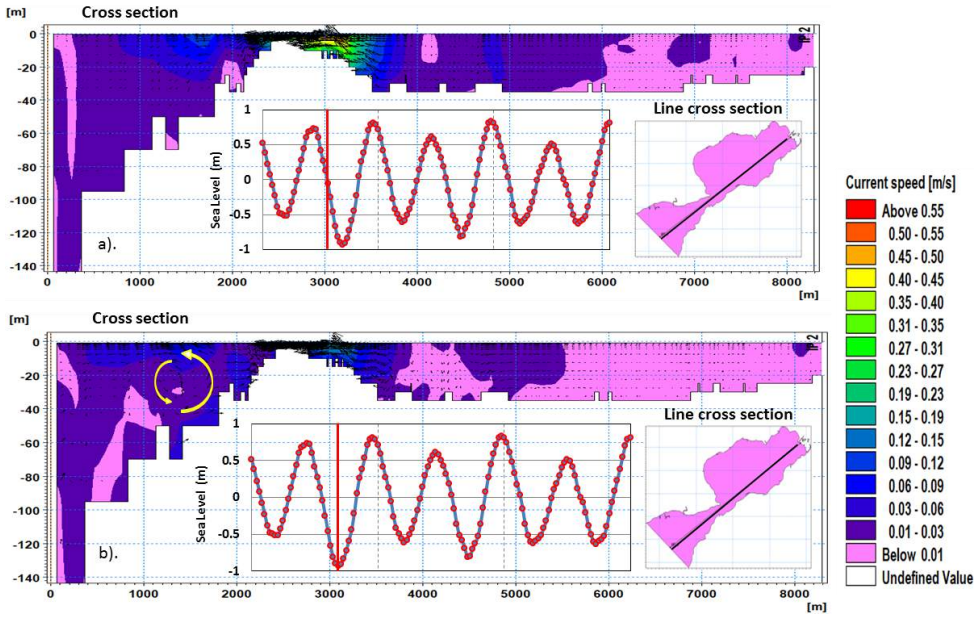

Figure 9: the Cross section of rainy season; a. ebb tide, b. low tide

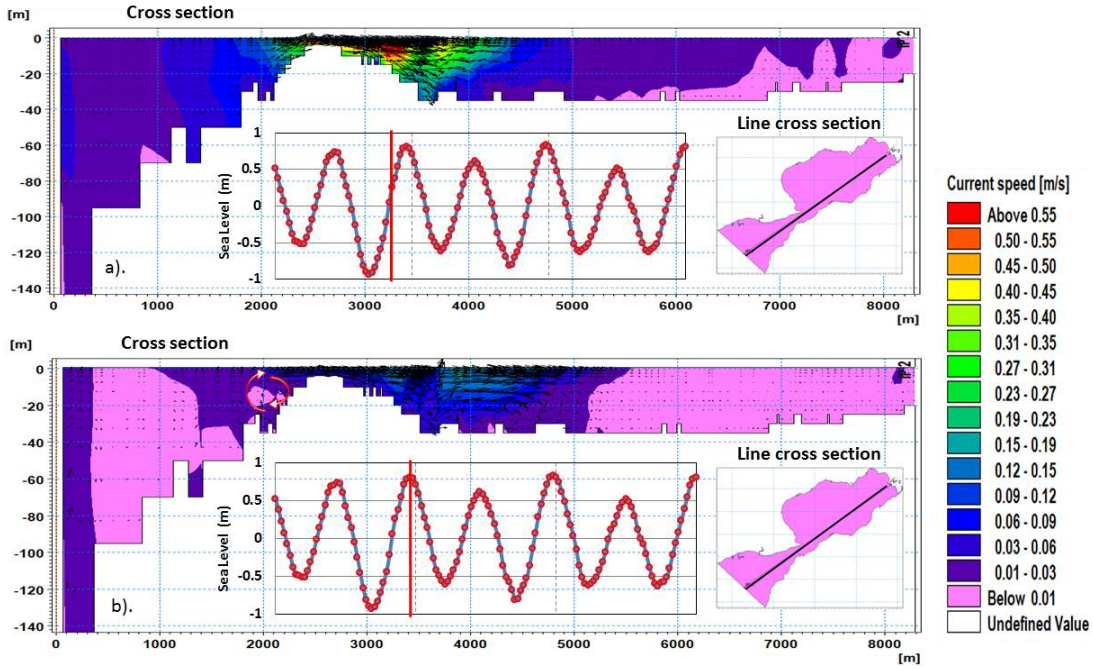

Figure 10: the Cross section of rainy season; a. flood tide, b. high tide

3.3 Simulation in dry season

In dry season the average of rainfall is about 3.2mm/day and make the average discharge inflow of 8 estuary into IAB is around 0.581m^3/s (Table 2). It seems that during dry season the discharge flow of rivers is not affect much the circulation of IAB, compering to the rainy seasons. Figure 11 shows during the phase of ebb tide the current flow in IAB has an average velocity of about 0.015m/s, which is slightly slower than those during the rainy season (Table 3). Current speed as it passes through the channel is between 0.5-0.35m/s or in averages about 0.246m/s, while the average current speeds at Ambon Bay about 0.023m/s. In general, the pattern of mass flow during the phase low ebb tide and low tide on dry season is similar to those on rainy season of the phase.

Figure 12a reveals that at low tide phase in surface layer of 0.25m there are five horizontal eddies. One of the eddy found in southeastern Ambon bay is anti-clockwise eddy (yellow arrow). In this phase the waters mass flow is exiting of the IAB and dominant flow passed the west side of Ambon bay, while on the southeast side, the flows was already started the phase of flood tide (it means the waters mass is flowing into IAB). This phenomenon perhaps driven the horizontal eddy causes the flow towards the channel, mostly turns direction and following the dominant flow which is exit from IAB. The other four horizontal eddy that exist in the IAB are found in the middle of bay, around Passo waters between Halong-Lateri (three anti-clockwise eddies (yellow arrow), and one clockwise-eddy (red arrow) around Hunut waters. The sum of horizontal eddy found in dry season is bigger than those in rainy season. At

10m depths the horizontal eddy in the waters between Halong and Lateri are disappeared. This phenomenon perhaps cause of the narrowing of topography towards the sea (Figure 12b). At depth of 20m, there are only two horizontal eddies left which are found in Passo waters (end of bay) and near of Hunut waters (Figure 12c). Probably, influence of inflow a rivers is affect to the circulation current flow rather strong in the rainy season, while in the dry season the current flow is only affected by the parameters of hydrodynamics and topography complexity. The horizontal eddy that occurs in IAB is probably affected by topography. In research of circulation in the Gulf of Patras (Greece); Conclude the influences of the internal wave and the tidal current mainly generate the eddies in Gulf [31, 32]. Furthermore, in the Bay of Biscay the model result shows the exchange flow indicated by the action of the tide and topography configuration [38, 39].

At phase of flood tide (Figure 13) shows the flow velocity at the channel is only around 0.4-0.2m/s on surface layers (0.25m) to 10m of depth (Figure 13a, 13b). Although, the flow velocity is slower in dry season, this flow entering to IAB passing thru the sill and the flow velocity force is sufficient to forming the horizontal eddy at 20m of depth (Figure 13c). In general, the average of flow velocity on IAB higher at rainy seasons is about 0.021m/s and in dry seasons is rather slower about 0.013m/s (Table 3). The flow velocity in IAB probably is influenced by proportions of current speed that entering through the channel. Figure 14 at phase high tide in surface layer 0.25m to 10m, it shows there are three horizontal eddy i.e. two anti-clockwise eddy (yellow arrow) in middle of bay and around Passo waters, and one clockwise eddy (red arrow) in Hunut waters (Figure 14a, 14b). While at 20m depth the horizontal eddy around Passo waters was disappeared (Figure 14c) probably due to the narrow topography and slowing flow velocity. Mostly, in this phase have same pattern in the rainy season, but a bit slower.

The cross sections (Figure 15) are in phase of ebb tide and low tide. Distance of barotropic conditions in ebb tide around 4060m (Figure 15a) is shorter than during the rainy seasons (Table 3). While in the low ebb the distance of barotropic condition is around 3060m and (Figure 15b) it shows two vertical anti-clockwise eddy (yellow arrow). First vertical eddy is in 40 of depth in front of the channel (at Ambon Bay) occurs probably due to the water mass flow at southeast Ambon bay (already start the flood tide phase) and the current flow heading into IAB (see Figure 12a). The inflow at 40m of depth collide with an increasingly topography as it near of channel, most of the flow swooping up (forming vertical eddy in Ambon bay) and partly passes along the east side of sill into the IAB (forming vertical eddy in IAB). The cross section at phase flood tide (Figure 16a) shows the distance of barotropic condition is about 3560m. While in phase of high tide (Figure 16b) show the eddy clockwise vertical (red arrow) in 20m of depth at Ambon bay and in near of sill in IAB, the patterns is exactly same as on vertical eddy at rainy seasons (Figure 14b). Other vertical eddy also happen on IAB (in middle of bay) with distance of barotropic condition is 3040m (Table 3).

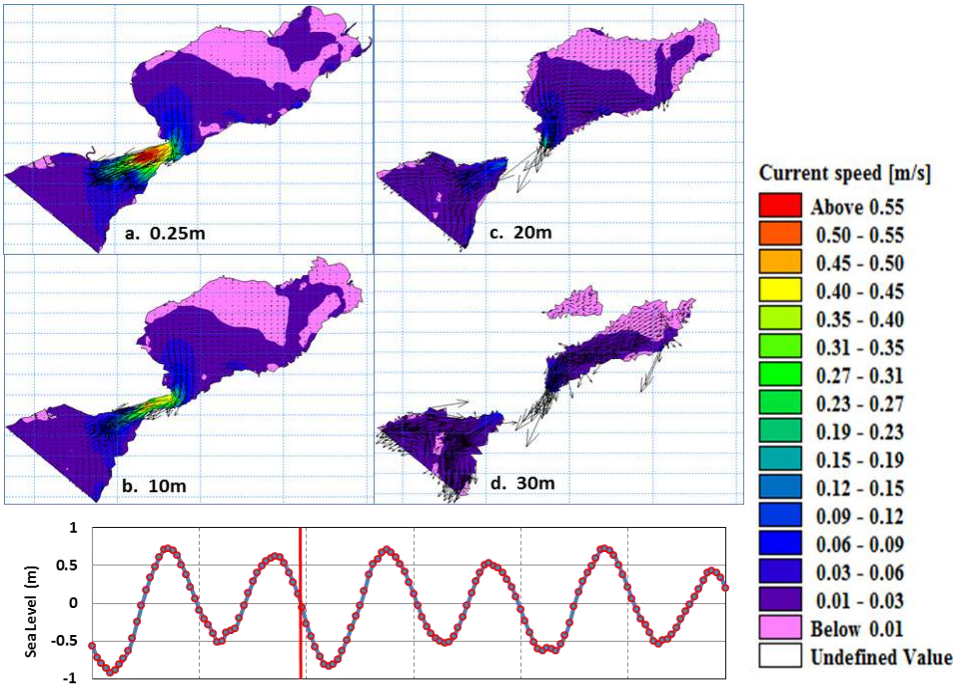

Figure 11: Current speed in the dry season, phase ebb tide (in the depth of): a). 0.25m, b). 10m, c). 20m, d). 30m

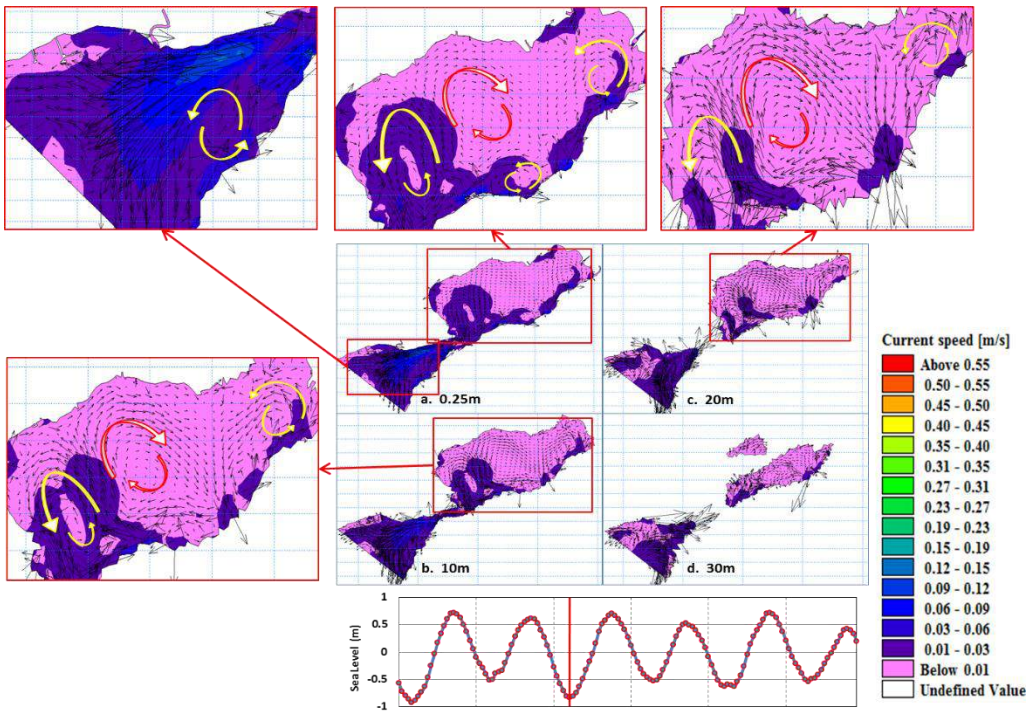

Figure 12: Current speed in the dry season, phase low tide (in the depth of): a). 0.25m, b). 10m, c). 20m, d). 30m

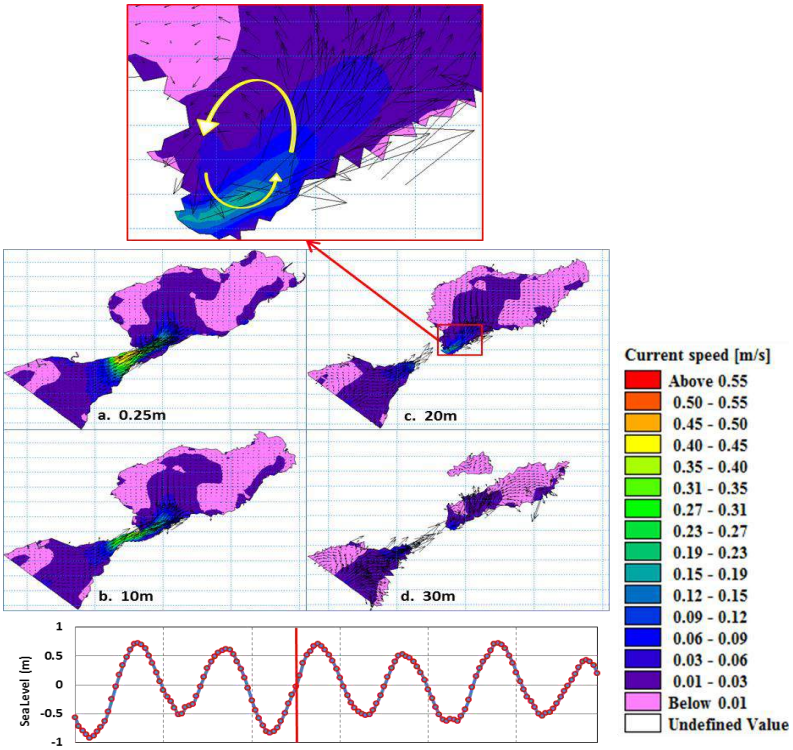

Figure 13: Current speed in the dry season, phase flood tide (in the depth of): a). 0.25m, b). 10m, c). 20m, d). 30m

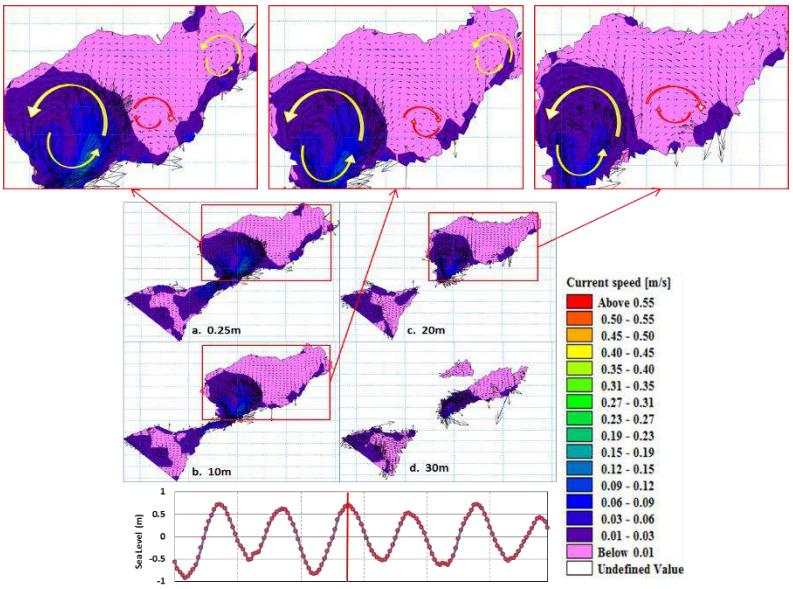

Figure 14: Current speed in the dry season, phase high tide (in the depth of): a). 0.25m, b). 10m, c). 20m, d). 30m

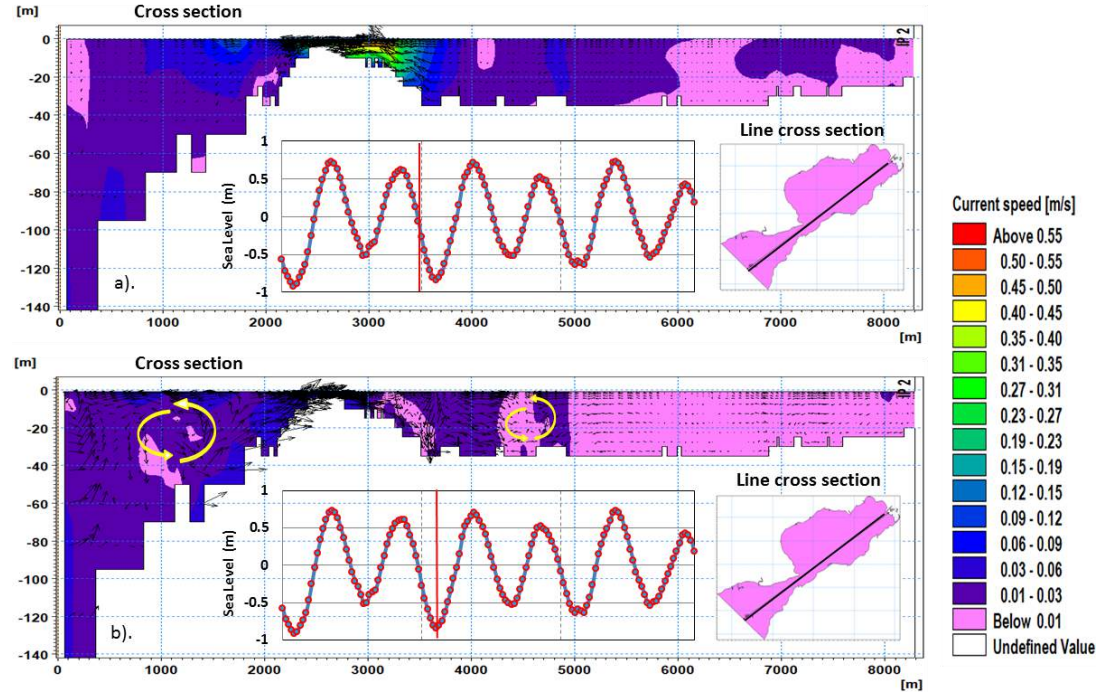

Figure 15: the Cross section of dry season; a. ebb tide, b. low tide

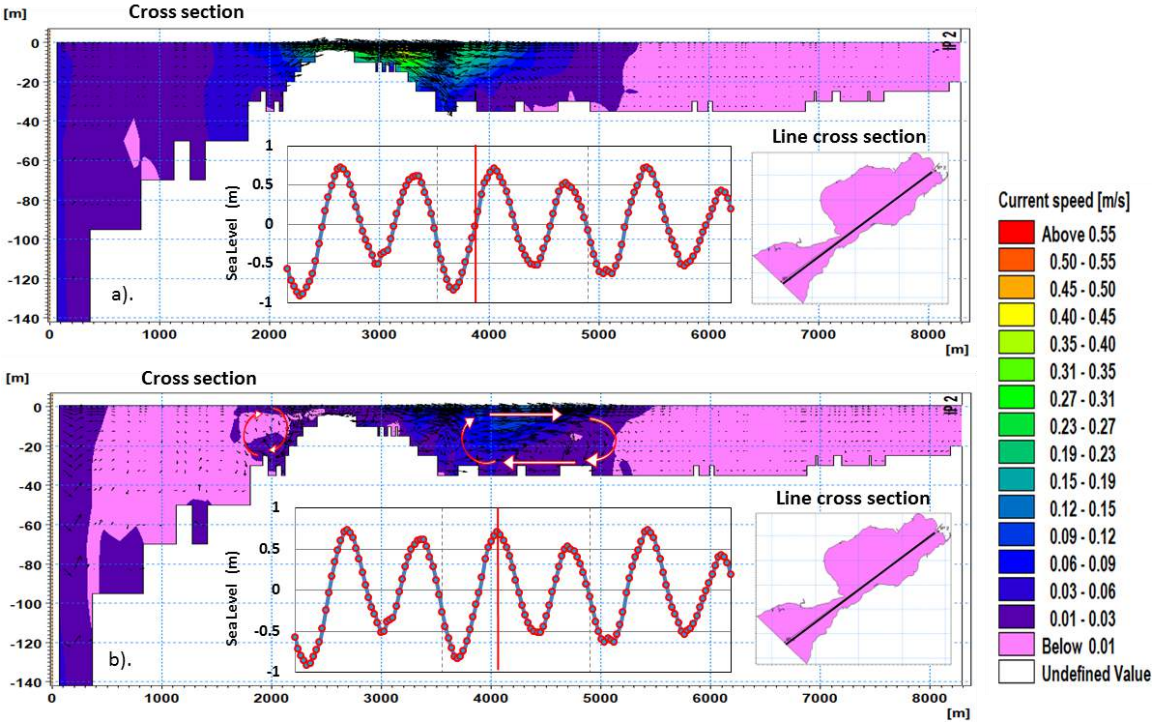

Figure 16: the Cross section of dry season; c. flood tide, d. high tide

IV. CONCLUSIONS

The 3-D finite volume hydrodynamic model, MIKE 3 FM, was implemented to barotropic circulation patterns to model the circulation of IAB and shows the results of it is well match with the parameters verification. At phase of ebb tide and low tide the water mass flow will leave IAB, while in phase of flood tide and high tide the water mass flow will enter to IAB. On the channel of bay the flow velocity reach maximum value which is suspected due to the flow compression affected by topography.

The simulation model result shows at phase of low tide and high tide the horizontal eddy more abudance than in ebb tide and flood tide. In seasonally, the number of horizontal eddy during the dry season is more considerable comparing to the rainy seasons. The parameters discharge of rivers (estuary) is suspected the main factors which influence the circulation and eddy patterns in IAB at rainy seasons. While during the dry seasons, the configuration of topography and tide parameters is probably the main factors which generate the eddys in IAB. Anti-clockwise horizontal eddy is dominant occur in the middle of bay and around Passo waters, while clockwise eddy horizontal predominantly happening in the waters between Batu koneng to Hunut. Based on the cross section, event of the anti-clockwise vertical eddy dominant at the low ebb phase, and in phase high tide the clockwise vertical eddy occured. The maximum distance of barotropic condition occurs in phase of low tide. Barotropic condition generally occurs when mass flow of waters being far from the sill and deepest spot of bay is at distance between 3000-4000m towards the edge of bay. It needs a further study on baroclinic condition in other to lern more about the circulation around to the threshold of the bay.

ACKNOWLEDGMENTS

Authors would like to thank Dr. Budi Wiryawan as head-office of DHI-Indonesia that already allow authors to use the MIKE 3 FM models in this research. Authors give appreciation to NUFFIC thru MDF-Indonesia in Bali for financial support of education and research.

REFERENCES

[1] Watttimury J.J, and Tuhumury S.F, 2003, “Vertical distribution characteristics of physical and chemical factors in waters of Inner Ambon dan Baguala Bay on December 2002”, Ichthyos, 4(1): pp.1-8.

[2] Tobalawony S., Tuahattu J.W., Wattimena S.M., 2009, “Physical characteristics of waters surface mass at Ambon Bay Waters in July”, Ichthyos, 8(1): pp. 35-41.

[3] Syahailatua A., 1999, “Komunitas fauna ikan yang tertangkap dengan jaring pantai dan bagan di Teluk Ambon Dalam : 1995-1997”, Oseanologi Indonesia, (31): pp. 41-55.

[4] Tarigan M.S, Edward., 2000, "Seasonal changes of temperature, salinity, dissolved oxygen, phosphate, and nitrate in Ambon Bay, Pesisir dan pantai Indonesia : Pusat penelitian dan pengembangan oseanologi", Lembaga ilmu pengetahuan Indonesia, Jakarta, pp. 73-86.
[5] Selnno D.A.J., 2009, "The analysis between the pollution load and the concentration of pollution as a basic management of aquatic environmental quality of Ambon Bay, Disertasi, Bogor Agricultural University, pp. 399.
[6] Hermanto B., 1987, "Laju sedimentasi dan stratifikasi sedimen Teluk Ambon Bagian Dalam", Balai penelitian dan pengembangan sumberdaya laut, Teluk Ambon; biologi, perikanan, oseanografi, dan geologi, 1987. pp. 125-132.
[7] Tuhumury N.Ch., Sahetapy J.M.F, Louhanapessy D.G., 2007, "Permasalahan Sedimentasi dan Pengelolaannya di Pesisir Lateri Kota Ambon", Jurnal Penelitian Ilmu-ilmu Perikanan dan Kelautan, 6(1): pp. 17-22.
[8] Suyadi., 2009, "The Condition of mangrove forest in Ambon Bay: prospect and challenges", Berita Biologi, 9(5): pp. 481-490.
[9] Tuhumury S.F., 2008, "The Community status of sea grass ini coastal water of Inner Ambon Bay", Ichthyos, 7(2): pp. 85-88.
[10] Cesar G.P., Guillermo D.R., Manuel R.V., Ricardo F.S., Christian M., 2012, "Circulation patterns at Le Danois Bank, an alongated shelf-adjacent seamount in the Bay of Biscay", Deep-Sea Research I, (60): pp. 7-21.
[11] Marinone S.G, and Mateos E, 2013, "Circulation in the deep canyon at the entrance to Todos Santos Bay, Mexico, is there a deep net outflow", Continental Shelf Research, (69): pp. 17-20.
[12] Arnaud L.B., Guillaume C., Bernard L.C., Pascal L., Louis M., 2013, "Circulation on the shelf and the upper slope of the Bay of Biscay", Continental Shelf Research, (55): pp. 97-107.
[13] Almudena F., Jon S., Manue G., Anna R., Ganix E., Julien M., Pedro L., Carlos H., Unai G., Michael C., 2013, "Coastal water circulation response to radiational and gravitational tides within the southeastern Bay of Biscay", Journal of Marine Systems, (109-110): pp. 95-104.
[14] Hearn C.J, and J.R Hunter.,1990, "A note on the equivalen of some two- and three-dimension models of wind-driven barotropic flow in shallow seas", Appl. Math. Modelling, (14): pp. 553-556.
[15] Argote M.L, M.F Lavin, and A. Amador., 1998, "Barotropic eulerian residual circulation in the Gulf of California due to the M_2 tide and wind stress", Atmosfera, (11): pp. 173-197.
[16] Xiaochun W., Yi C., Changming D., John F., Zhijin L., James C.M., Jeffrey D.P., Leslie K.R., 2009, "Modeling tides in Monteret Bay, California, Deep-sea Research II, (56): pp. 219-231.
[17] Daji H, Jilan S, and Jan O.B., 1999, "Modelling the seasonal thermal stratification and baroclinic circulation in the Bohai Sea", Continental shelf Research, (19): pp. 1485-1505.
[18] Guoqi H., Zhimin M., Brad Y., Mike F., and Nancy C., 2011, "Simulation of three-dimension circulation and hydrography over the Grand Banks of Newfounland", Ocean Modelling, (40): pp. 199-210.

[19] Antonio M.B., Yinglong Z., Arun C., Mike Z., Charles S., Edward P.M., John K., Michale W., Michael B., Paul J.T., 2005, "A cross-scale model for 3D baroclinik circulation in estuary-plume-self systems: II. Application to the Colombia river", Continental shelf research,(25): pp. 935-972.
[20] Dong W.J., HyoSeon P., SeongJoon B., and Jin T.C., 2005, "A study on the water gate operation in the canal sytem bay MIKE 3 FM", International journal of control and automation, 8(1): pp. 157-168.
[21] Rhony E.R., Hadi S.A., Cecep K., and Alex S.W.R., 2015, "Contribution of Dusun Agroforestry to Household Income on Ambon Island, Indonesia", International Journal of Sciences: Basic and Applied Research, 23(1): pp. 256-267.
[22] Hamzah M.S, dan Wenno L.F., 1987, "Sirkulasi arus di teluk ambon", Balai penelitian dan pengembangan sumberdaya laut, Teluk Ambon; biologi, perikanan, oseanografi, dan geologi, pp. 91-101.
[23] Hatayama T., Toshiyuki A., and Kazunori A., 1996, "Tidal Current in Indonesia Seas and their effect on transport and mixing", Journal of Geophysical Research, (C5): pp. 12353-12373.
[24] DHI, MIKE 21 & 3 Flow Model FM ; hydrodynamic and Transport Module, 2012, "Scientific Documentation, DHI-Denmark, pp.58.
[25] Pin Li., Guangxue Li, Lulu Qiao, Xueen C., Jinghao S., Fei G., Nan W., Shuhong Y., 2014, "Modeling the tidal dynamic change by the brige in Jiazhou bay, Qingdao, China", Continental shelf research, (84): pp. 43-53.
[26] Xing Wei, Peitong Ni, and Haigang Zhan, 2013, "Monitoring cooling water discharge using lagrangian choherent structures: a case study in Daya Bay, China", Marine pollution bulletine, pp. 105-113.
[27] Alan F. K. and Motoyoshi I., 2008, "Three-dimensional of tidal circulation and mixing over the Java Sea", Journal of Oceanography, (64): pp. 61-80.
[28] Wenno L.F. and Anderson J.J., 1983, "Evidence for tidal upwelling across the sill of Ambon Bay", Mar. Res. Indonesia, (23): pp. 13-20.
[29] Wenno L.F., 1991, "Notes on the optical properties of Ambon Bay", Perairan Maluku dan sekitarnya, 1991. pp. 105-112.
[30] Wagey G.A, 2002, "Ecology and physicology of phytoplankton in Ambon Bay, Indonesia", Doctor Disertation. The University of Britush Columbia, pp. 184.
[31] Nikolaos Th.F. and Georgios M.H., 2012, "Early summer circulation in the Gulf of Patras (Greece)", Proceeding of International offshore and polar engineering conference, pp. 740-745.
[32] Androniki K., Georgios M.H., and Nikolaos Th.F., 2015, "Hydrodynamic circulation and hydraulic exchange in the Pappas lagoon, western Greece", Proceeding IAHR World Congress - Netherlands, pp. 1-8.
[33] Hunt J.C.R. and Jackson P.S., 1974, "Wakes behind two-dimensional surface obstacle in turbulent boundary layers", Journal Fluid Mechanic, 64(3): pp. 529-563.
[34] Ozgokmen T.M, Chassignet E.P., and Paiva A.M., 1997, "Impact of wind forcing, bottom topography, and inertia an Midlatitude jet separation in a

quasigeostropihic model", Journal of physical oceanography, (27): pp. 2460-2476.

[35] Jiang L., Yan X.H, Tseng Y.H, and Breaker L.C., 2011, "A numerical study on the role of wind forcing, bottom topography, and nonhydrostacy in coastal upwelling", Esuarine, coastal and shel science, (95): pp. 99-109.

[36] Marchesiello, Mcwilliams P., and Shchepetkin J.C., 2003, "Equlibrium structure and dynamics of the California current system", Journal of physical oceanography, 33(4): pp. 753-783.

[37] Pingree R.D, and B. Le Cann, 1992, "Three andtycyclonic slope water oceanic eddies (swoddies) in the southern Bay of Biscay in 1990", Deep sea research, (39): pp. 1147-1175.

[38] Ferrer L. and Caballero A., 2011, "Eddies in the bay of Biscay: a numerical approximation", Journal of marine system, (87): pp. 133-144.

[39] Caballero A., Luis F., Anna R., Guillaume C., Benjamin H. T., and Nicolas G., 2014, "Monitoring of quasi-stasionary eddy in the Bay of Biscay by means of satellite, in-situ, and model results", Deep sea research part II: Tropical studies in oceanography, (106): pp. 23-37.